IET Control Theory & Applications

Research Article

IET Journals
The Institution of Engineering and Technology

Air–fuel ratio control of lean-burn SI engines using the LPV-based fuzzy technique

ISSN 1751-8644
Received on 1st March 2017
Revised 7th February 2018
Accepted on 2nd March 2018
E-First on 12th April 2018
doi: 10.1049/iet-cta.2017.0063
www.ietdl.org

Hsiu-Ming Wu[1] ✉, *Reza Tafreshi*[2]

[1]*Department of Mechanical Engineering, National Chin-Yi University of Technology, Taichung, Taiwan*
[2]*Mechanical Engineering Program, Texas A&M University at Qatar, Doha 23874, Qatar*
✉ *E-mail: wu.hsiu.ming@gmail.com*

Abstract: Control of air–fuel ratio (AFR) plays a key role in the minimisation of the carbon dioxide and harmful pollutant emissions and maximisation of fuel economy. An inherent time-varying delay existing in lean-burn spark ignition (SI) engines is a major challenge for the AFR control. Herein an unstable internal dynamics with a parameter dependent system caused by time delay is established to represent a dominating feature of AFR. The proposed control scheme, LPV-based fuzzy control technique, combines the features of LPV and fuzzy control to deal with the unstable internal dynamics of an AFR system with external disturbances and a high level of uncertainty in system parameters. Based on the desired error dynamics, an LPV dynamic error consisting of the unstable state and the AFR tracking error is determined. Subsequently, the proposed fuzzy control algorithm through a look-up table is used to stabilise the LPV dynamic error. Then, the tracking error moves along the desired error dynamics towards zero. The system stability is assured via Lyapunov stability criteria. Finally, the simulation results demonstrate the effectiveness and robustness of the proposed control scheme under different operating conditions. Also, compared with the baseline controller, i.e. proportional–integral controller with Smith predictor, demonstrates its superiority.

1 Introduction

Due to the environmental and economic concerns, lean-burn technology has attracted a lot of attention from engineers and scientists around the world. Lean-burn spark ignition (SI) engines operate at a relatively high air–fuel ratio (AFR) value, i.e. higher than stoichiometric value, resulting in less fuel consumption, and producing less carbon dioxide emission. Consequently, a good balance between fuel efficiency, power output, and pollution emission can be obtained. A lean NOx trap (LNT) module integrated with the three-way catalyst (TWC) in SI engines is typically constructed so that the NOx pollutants can be converted into non-polluting nitrogen. In general, it usually takes a long time for the air–fuel mixture to reach the universal exhaust gas oxygen (UEGO) sensor downstream the LNT module (Fig. 1) during this process. This large time delay, which is also varying, becomes the main challenge for the control of AFR. A large time-varying delay will shorten the bandwidth of the closed-loop system and degrade the system performance. In addition, it may even create instability and cause the controller design to become a challenging task.

Since the last decade, researchers have been continuously proposing different approaches to resolve this time-varying related issue for efficient controlling of AFR system. The most important findings from these studies will be discussed here. Muske *et al.* [2] proposed an adaptive and model-predictive controller for SI engine AFR control. The model states and the system disturbance were estimated by a Kalman filter. Shortly after, Tang *et al.* [3] presented an adaptive and learning control approach for multi-input and multi-output engine models with constant and time-varying uncertainties. Moreover, an adaptive control method of time-delay systems applied to SI internal combustion (IC) engine was also proposed by Yildiz *et al.* [4]. This approach considered two adaptive controller designs; one based on feedforward adaptation while the other one was based on both feedback and feedforward adaptation incorporating adaptive posicast controller. Besides, Chen *et al.* [5] proposed a linear quadratic optimal tracking controller based on the adaptively estimated biofuel content to track the desired AFR for a lean burn SI engine. Further, in [6, 7], an adaptive internal model control for AFR control was proposed to adapt the unknown time constant of the system plant with a time-varying delay (that makes the AFR system a parameter dependent system), and uncertain disturbances. Recently, Khajorntraidet *et al.* [8] proposed an adaptive algorithm with Smith predictor to estimate the time delay in port injection engines. The above studies all adopted adaptive control strategies for AFR control. As ones know, the adaptive control may cause a larger transient response and even instability in the face of a large and time-varying delay. In other words, adaptive control may not be a good solution for AFR control with a large time-varying delay. Moreover, two more control structures were proposed to solve this problem: an observer-based fuel-injection control strategy in [9] and a non-linear control method based on Takagi–Sugeno modelling of an AFR system with a variable time delay in [1].

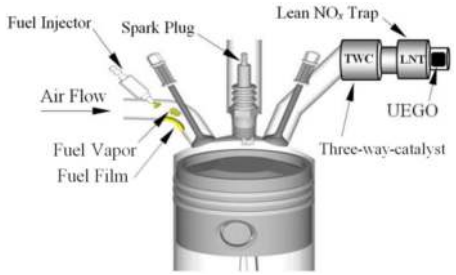

Fig. 1 *Schematic description of the air-fuel path in an SI engine adopted from [1]*

In this work, a parameter dependent system caused by an AFR system with time-varying delay is obtained by means of Pade approximation and normal form transformation. A suited approach, i.e. a linear parameter-varying (LPV) technique for the parameter dependent system was proposed. Details of the stability analysis for this approach can be found in [10]. The following is a representative few of the LPV technique applying to an AFR system. Zhang *et al.* [11] demonstrated satisfactory stability and disturbance rejection performance using an LPV control system for the AFR control of a lean-burn SI engine in the presence of the time-varying delay. Ebrahimi *et al.* proposed a second-order sliding mode [12] and a parameter-varying filtered PID strategies [13] for AFR control of lean-burn engines. The authors reported that their

proposed methods could effectively remove the effects of time-varying delay, canister purge disturbance, and measurement noise. Postma and Nagamune [14] used a switching LPV controller for a time-varying first-order-plus-dead-time model, which was found by solving a convex optimisation problem with linear matrix inequalities (LMIs). Tafreshi *et al.* [15] developed a linear dynamic parameter-varying sliding manifold based on unstable internal dynamics to control the AFR. Yin and Liu [16] proposed a gain-scheduled delay-dependent controller, regarding the time delay as a time-varying parameter, to track AFR reference and minimise the effect of disturbances.

These above studies demonstrated that an LPV technique is capable of effectively coping with an AFR system along with large time-varying delay for the AFR control system. Moreover, having a robust controller combined with the LPV technique for the AFR system is very important to tackle the issues associated with unknown and uncertain disturbances, issues – such as unmodelled dynamics and Pade approximation error. Since the LPV technique sufficiently demonstrated the capacity to deal with time-varying related challenges and a fuzzy control has characteristics of the model-free and high level of robustness, we proposed an LPV-based fuzzy control scheme in this work to combine the advantages of both of these methods. To the best of our knowledge, an LPV-based fuzzy control has not been previously introduced for such time-varying systems. We hypothesised that the developed scheme would effectively handle the parameter-dependent problem to stabilise the AFR system as it incorporates both model-free principle and highly robust control features. In summary, the contributions of this paper include approximating the AFR system using first-order Pade technique, obtaining an unstable internal dynamics via the norm form transformation, constructing an LPV approach including unstable state and AFR tracking error with the desired dynamics, and designing a highly robust fuzzy controller through the development of a look-up table to stabilise the LPV dynamic error and control AFR performance.

The paper is organised as follows: an AFR dynamics is represented and AFR control problem is stated in Section 2. In Section 3, the LPV-based fuzzy control design is described and its stability is proved. Simulation results and discussions are presented in Section 4. Finally, in Section 5 some conclusions are made.

2 AFR dynamics and problem statement

In this section, an AFR dynamics characterised by a time-varying delay and its internal dynamics are presented. In the following stage, the problem statement on AFR control of a lean-burn engine system is described. Fig. 1 depicts a typical SI engine system including throttle, air path, fuel path, TWC, LNT and UEGO sensor. The AFR is determined by the air-flow passing through the intake manifold and the fuel injected by the fuelling system. In general, the normalised AFR can be defined as $\mathrm{AFR} = \dot{m}_\mathrm{a}/(\dot{m}_\mathrm{f}\mathrm{AFR}_\mathrm{s})$, where $\dot{m}_\mathrm{a}$ and $\dot{m}_\mathrm{f}$ are the air and fuel mass flow rates, respectively [17]. The stoichiometric value of AFR (AFR_s) is approximately 14.7 for gasoline engines [18]. The AFR that is lower than this stoichiometry value is known as a lean mixture.

2.1 AFR dynamics

A time-varying delay plays a key role in modelling the AFR dynamics of lean-burn SI engines, where larger the time-varying delays higher the difficulties in tracking the AFR. During the engine control loop, this time-varying delay can be broken in two parts: (i) the cycle delay (τ_c) due to the four strokes of the engine, which can be expressed as $\tau_\mathrm{c} = 720/(360/60)v = 120/v\,[s]$ where v denotes the engine speed in RPM, and (ii) the gas transport delay (τ_g) to the UEGO sensor, which can be expressed as $\tau_\mathrm{g} = \alpha/\dot{m}_\mathrm{a}$, where α is usually determined from the experimental data. The resultant total time delay $\tau = \tau_\mathrm{c} + \tau_\mathrm{g}$, varies depending on the engine operating condition. Therefore, the AFR path from the fuel injector to the UEGO sensor can be approximated by a first-order lag with a delay [19–22] as

$$\tau_\mathrm{s}\dot{y}(t) + y(t) = u(t-\tau) \tag{1}$$

where $y(t)$ and $u(t)$ are the measured and control input AFRs, respectively, and τ_s is the UEGO time constant [1]. The infinite dimensional time delay term in open-loop system dynamics may be approximated by the Pade approximation, as a finite-dimensional closed-form representation. Using a first-order Pade approximation, (1) can be rewritten in transfer function form as

$$\frac{Y(s)}{U(s)} \cong \frac{1-(\tau/2)s}{(1+(\tau/2)s)(1+\tau_\mathrm{s}s)} \tag{2}$$

This transfer function is a non-minimum phase system due to the presence of zeros in the right-half plane that is caused by the time delay. Its state-space representation can be expressed as

$$\begin{cases} \dot{x}_1(t) = x_2(t) \\ \dot{x}_2(t) = -a_0(\tau)x_1(t) - a_1(\tau)x_2(t) + u(t) \\ y(t) = b_0(\tau)x_1(t) + b_1(\tau)x_2(t) \end{cases} \tag{3}$$

where $a_0(\tau) = b_0(\tau) = 2(\tau_\mathrm{s}\tau)^{-1}$, $a_1(\tau) = (2\tau_\mathrm{s}+\tau)(\tau_\mathrm{s}\tau)^{-1}$, and $b_1(\tau) = -\tau_\mathrm{s}^{-1}$ are the parameter dependent coefficients. Since the system is a non-minimum phase, we will be focusing on the control and stabilisation of the system's internal dynamics. Through the normal form transformation of $W = N(x(t))$, where $W = [\zeta(t) \quad \eta(t)]^\mathrm{T}$, $x(t) = [x_1(t) \quad x_2(t)]^\mathrm{T}$, and $N(x) = [y(t) \quad x_1(t)]^\mathrm{T}$ [7], the associated internal dynamics can be given using Lie notation as

$$\begin{aligned} \dot{\eta}(t) &= L_\mathrm{f}N(x(t)) \\ \dot{\zeta}(t) &= L_\mathrm{f}h(x(t)) + L_\mathrm{g}h(x(t))u(t) \end{aligned} \tag{4}$$

where $f(x(t)) = [x_2(t) \quad -a_0(\tau)x_1(t) \quad -a_1(\tau)x_2(t)]^\mathrm{T}$, $g(x(t)) = [0\ 1]^\mathrm{T}$, $h(x(t)) = b_0(\tau)x_1(t) + b_1(\tau)x_2(t)$, and $N(x(t))$ are found such that $L_\mathrm{g}N(x(t)) = 0$. Thus, internal dynamics of the AFR control system and input/output pairs are then expressed as

$$\begin{cases} \dot{\eta}(t) = a_{11}(\tau)\eta(t) + a_{12}\zeta(t) + \phi_\eta(t) \\ \dot{\zeta}(t) = a_{21}(\tau)\eta(t) + a_{22}(\tau)\zeta(t) + \beta u(t) + \phi_\zeta(t) \\ y(t) = \zeta(t) \end{cases} \tag{5}$$

where $\eta(t)$ and $\zeta(t)$ are, respectively, state variables, $a_{11}(\tau) = 2\tau^{-1}$, $a_{12} = -\tau_\mathrm{s}$, $a_{21}(\tau) = (8\tau_\mathrm{s}+4\tau)(\tau_\mathrm{s}\tau)^{-2}$, $a_{22}(\tau) = -(4\tau_\mathrm{s}+\tau)(\tau_\mathrm{s}\tau)^{-1}$, and $\beta = -\tau_\mathrm{s}^{-1}$ are corresponding coefficients in terms of the above transformation; $\phi_\eta(t)$ and $\phi_\zeta(t)$ represent the bounded external disturbances. Evidently, the zero dynamics in (5) is unstable due to the variable coefficient, $a_{11}(\tau) > 0$. Therefore, designing a parameter-dependent controller with a high level of robustness is essential to deal with such an unstable system with variable parameters. In the following subsection, the specific control problem for the AFR system is described.

2.2 Problem statement

Due to the large time-varying delay and the effect of external disturbances and uncertainty, AFR control is a challenging task. An LPV-based fuzzy controller design with a high level of robustness is advantageous to control the AFR. In order to apply the LPV approach, system dynamics needs to be known in advance. In this paper, it is assumed that the two parameters of AFR internal dynamics in (5), i.e.$a_{11}(\tau)$, and a_{12} are known. The control objective is to design the control input $u(t)$ (i.e. LPV-based fuzzy control) such that the system output $y(t)$ asymptotically converges to the desired AFR, $y^*(t)$ within a finite time, despite the presence of bounded disturbances as well as the uncertainty in system parameters. In the control loop, an LPV dynamic error is constructed and then a fuzzy control algorithm based on a look-up

table is used for the AFR internal dynamics. The overall control configuration is shown in Fig. 2.

3 LPV-based fuzzy controller design and stability proof

In this section, first, an LPV-based fuzzy controller is designed to track the desired AFR values under different operating conditions. Then, the stability of LPV-based fuzzy control system is proved.

3.1 LPV-based fuzzy controller design

In order to tackle the unstable parameter dependent system in (5), an LPV dynamic error $\chi(t)$ including the unstable state $\eta(t)$ and AFR tracking error $e(t) = y^*(t) - \zeta(t)$, is given as follows [10]:

$$\chi(t) = \eta(t) + \frac{\sum_{j=0}^{n-1} p_j(\tau)s^j}{s^{n+1} + q(\tau)s^n} e(t) = 0 \tag{6}$$

where $s = \mathrm{d}/\mathrm{d}t$ and n is a positive constant to determine the system order. The LPV coefficients $p_j(\tau)$ and $q(\tau)$ can be determined using the following desired error dynamics:

$$\left(s^{n+1} + \sum_{j=0}^{n} c_j s^j\right) e(t) = 0 \tag{7}$$

where c_j coefficients depends on the desired eigenvalue placement. Then, using this definition in (6), the motion dynamics of the LPV dynamic error along the internal dynamics in (5) yields

$$\begin{aligned} &\left\{s^{n+1} + q(\tau)s^n - a_{12}^{-1}\sum_{j=0}^{n-1} p_j(\tau)\left[s^{j+1} - a_{11}(\tau)s^j\right]\right\} e(t) \\ &\quad = \left\{a_{12}^{-1}\left[s^{n+1} + q(\tau)s^n\right]\right\}\bar{\phi}(t) \end{aligned} \tag{8}$$

where $\bar{\phi}(t) = a_{12}y^*(t) + \phi_\eta(t)$ is a bounded smooth function, whose kth-order time derivative is zero, i.e. $\left(\mathrm{d}^k/\mathrm{d}t^k\right)\bar{\phi}(t) \equiv 0$, and $k < n$. Therefore, the right-hand side in (8)becomes zero and the zero steady-state tracking error is achieved

$$\left\{s^{n+1} + q(\tau)s^n - a_{12}^{-1}\sum_{j=0}^{n-1} p_j(\tau)\left[s^{j+1} - a_{11}(\tau)s^j\right]\right\} e(t) = 0 \tag{9}$$

By rearranging (9) in descending order of derivatives and equating the corresponding coefficients with the desired characteristic equation of the tracking error in (7), the coefficients $q(\tau)$ and $p_j(\tau)$ are determined as

$$\begin{aligned} q(\tau) &= c_n + \sum_{j=0}^{n-1} a_{11}^{j-n}(\tau)c_j, \\ p_j(\tau) &= a_{12}\sum_{i=0}^{j} a_{11}^{i-j-1}(\tau)c_i \end{aligned} \tag{10}$$

Substitution of (10) into (6) represents the LPV dynamic error manifold as

$$\chi(t) = \eta(t) + \Phi(s)e(t) = 0 \tag{11}$$

where

$$\Phi(s) = \frac{a_{12}\sum_{j=0}^{n-1}\sum_{i=0}^{j} a_{11}^{i-j-1}(\tau)c_i s^j}{s^{n+1} + c_n s^n + \sum_{j=0}^{n-1} a_{11}^{j-n}(\tau)c_j s^n}$$

In addition, the time derivative is found as

$$\begin{aligned} \dot{\chi}(t) &= \dot{\eta}(t) + \Phi(s)\dot{e}(t) \\ &= a_{11}(\tau)\eta(t) + a_{12}\zeta(t) + \phi_\eta(t) + \Phi(s)\left[\dot{y}^*(t) - \dot{\zeta}(t)\right] \\ &= a_{11}(\tau)\eta(t) + a_{12}\zeta(t) + \phi_\eta(t) + \Phi(s)\dot{y}^*(t) \\ &\quad -\Phi(s)\left[a_{21}(\tau)\eta(t) + a_{22}(\tau)\zeta(t) + \beta u(t) + \phi_\zeta(t)\right] = 0 \end{aligned} \tag{12}$$

In this way, the LPV dynamic error $\chi(t)$ can be determined based on (9) such that the unstable state $\eta(t)$ in the AFR internal dynamics in (5) can be stabilised afterwards via the proposed fuzzy control. To manipulate the preceding LPV dynamic error towards zero, a fuzzy control based on a look-up table is proposed next. Note that the derivative of the LPV dynamic error is substituted with its difference, i.e. $\dot{\chi}(t) \simeq [\chi(mT_\mathrm{s}) - \chi(m-1)T_\mathrm{s}]/T_\mathrm{s}$ where m represents the mth step and T_s denotes the sampling time. In general, this time derivatives become more accurate when the sampling time is smaller. The derivative approximation error is regarded as part of the uncertainties. Fig. 3 depicts the proposed fuzzy control block diagram that maps $\left[\bar{\chi}(t) \quad \dot{\bar{\chi}}(t)\right]^\mathrm{T} \in X \subset \mathfrak{R}^2$ to $\bar{u}(t) \in V \subset \mathfrak{R}$ where $\bar{\chi}(t) = g_\chi\chi(t)$ and $\dot{\bar{\chi}}(t) = g_{\dot{\chi}}\dot{\chi}(t)$. The parameters g_χ and $g_{\dot{\chi}}$ are positive and chosen such that both $\bar{\chi}(t)$ and $\dot{\bar{\chi}}(t)$ are in $[-1, 1]$. Three main parts in Fig. 3 include fuzzifier, fuzzy inference engine based on a rule, and defuzzifier. The fuzzifier transfers crisp points $\bar{\chi}(t)$ and $\dot{\bar{\chi}}(t)$ into a fuzzy set in X using a membership function (Fig. 4); the fuzzy inference engine maps fuzzy sets in X to fuzzy sets in V, based on a set of IF–THEN rules in the fuzzy rule base and the compositional rule of inference; and the defuzzifier maps a fuzzy set in V to a crisp point in V through the same function.

In fuzzifier block, the fuzzy variables, i.e. crisp points $\bar{\chi}(t)$ and $\dot{\bar{\chi}}(t)$, are quantised into the following eleven qualitative fuzzy variables (i.e. $l = 11$): (i) positive huge (PH), (ii) positive big (PB), (iii) positive medium (PM), (iv) positive small (PS), (v) positive infinitesimal (PI), (vi) zero (ZE), (vii) negative infinitesimal (NI), (viii) negative small (NS), (ix) negative medium (NM), (x) negative big (NB), and (xi) negative huge (NH) (Table 1). However, it is not essential to select all these eleven fuzzy rules. A smaller fuzzy rule set (e.g. $l = 7$) may lead to an acceptable performance (e.g. [23]). While there are many types of membership functions exists in the literature such as bell shaped, trapezoidal shaped, and triangular shaped, we used the triangular type in this study (Fig. 4).

In this study, we introduced the following l fuzzy control rules where the upper script k denotes the kth fuzzy rule:

$$\text{IF } \bar{\chi}(t) \text{ is } F_1^k \text{ and } \dot{\bar{\chi}}(t) \text{ is } F_2^k, \text{ THEN } \bar{u}(t) \text{ is } H^k \tag{13}$$

where $\bar{\chi}(t)$ and $\dot{\bar{\chi}}(t)$ are the inputs and $\bar{u}(t)$ is the output of the fuzzy logic system; F_j^k and H^k $(1 \le j \le 2, 1 \le k \le l)$ are sets in X and V, respectively. The inference engine is activated by the relevant fuzzy rules to form the linguistic rule of the fuzzy control algorithm (Table 1). If $\left[\bar{\chi}(t), \dot{\bar{\chi}}(t)\right]$ lies on the diagonal of Table 1 (i.e. ZE), there is no control action, which is the case of keeping the states on a dynamic manifold. However, there are control actions of the upper triangle terms, i.e. NI to NH and on lower triangle terms, i.e., PI to PH that makes Table 1 skew-symmetric.

In practice, the linguistic term should be converted to a non-fuzzy value. Thus, the linguistic rule in Table 1 is defuzzified by employing the centre of gravity method to form a look-up table that directly relates the inputs $\bar{\chi}(t)$ and $\dot{\bar{\chi}}(t)$ to the output $\bar{u}(t)$ (Table 2). Table 2 has been designed such that $u(t)$ increases when $\dot{\chi}(t)$ increased. If $\chi(t) > 0$, then decrease of $u(t)$ will result in a decrease of $\chi(t)\dot{\chi}(t)$. However, if $\chi(t) < 0$, then the increase of $u(t)$ will results in a decrease of $\chi(t)\dot{\chi}(t)$. In other words, Table 2 has been generated to satisfy $\chi(t)\dot{\chi}(t) < 0$ via $u(t)$, which results in the decrease of Lyapunov function, i.e. $\dot{V}(t) < 0$.

Based on the aforementioned discussion, Table 2 can be summarised as

$$u(t) = g_u\bar{u}(t) = g_u\{\bar{\chi}_\tau(t) + \Delta(t)\mathrm{sgn}(\bar{\chi}_\tau(t))\} \tag{14}$$

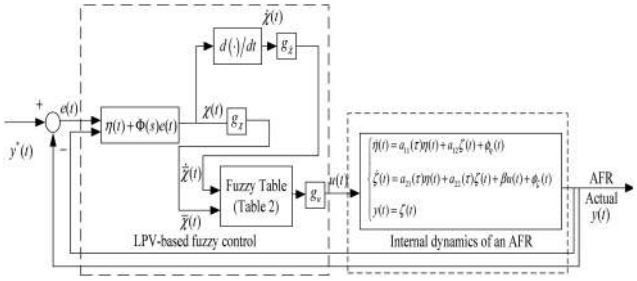

Fig. 2 *Proposed LPV-based fuzzy control block configuration*

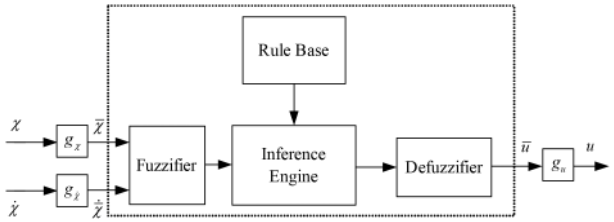

Fig. 3 *Proposed fuzzy control block diagram*

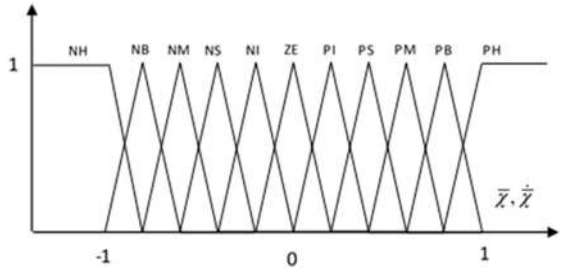

Fig. 4 *Membership functions with triangular type*

where $\bar{u}(t)$ is the fuzzy variable of $u(t)$; $\Delta(t) < 0$ denotes a switch gain, which is obtained from Table 2 depending on $\bar{\chi}(t)$ and $\dot{\bar{\chi}}(t)$, $\forall t$; $\bar{\chi}_\tau(t) = \bar{\chi}(t - \tau(t))$ and $\tau(t)$ denotes a time-varying delay with an upper bound, τ_u, and g_u is the output scaling factor satisfying the following inequality:

$$g_u \geq \frac{|f(t)| + \lambda / g_\chi}{\Phi(s)\beta\Delta(t)} \tag{15}$$

where $\lambda > 0$ is a positive constant; and $f(t)$ is defined as

$$\begin{aligned} f(t) = {} & a_{11}(\tau)\eta(t) + a_{12}\zeta(t) + \phi_\eta(t) + \Phi(s)\dot{y}^*(t) \\ & - \Phi(s)a_{21}(\tau)\eta(t) - \Phi(s)a_{22}(\tau)\zeta(t) \\ & - \Phi(s)\beta g_u \bar{\chi}_\tau(t) - \Phi(s)\phi_\zeta(t) \end{aligned} \tag{16}$$

Although the risk of the transient response may happen, we choose a larger output scaling factor g_u since it results in a smaller tracking error and a faster response.

In the next subsection, it is shown that once the inequality in (15) is satisfied, the LPV dynamic error in (11) becomes asymptotically stable. Further, the tracking error becomes asymptotically stable under the action of the proposed LPV-based fuzzy control.

3.2 Stability proof

The Lyapunov function is defined as

$$V(t) = \bar{\chi}^2(t)/2 > 0, \quad \text{as } \bar{\chi}(t) \neq 0. \tag{17}$$

Taking its time derivative and substituting (12) into (17) yielded

Table 1 Fuzzy control rules

$\dot{\bar{\chi}}$ \ $\bar{\chi}$	PH	PB	PM	PS	PI	ZE	NI	NS	NM	NB	NH
NH	ZE	NI	NS	NM	NM	NB	NB	NB	NH	NH	NH
NB	PI	ZE	NI	NS	NM	NM	NB	NB	NB	NH	NH
NM	PS	PI	ZE	NI	NS	NM	NM	NB	NB	NB	NH
NS	PM	PS	PI	ZE	NI	NS	NM	NM	NB	NB	NB
NI	PM	PM	PS	PI	ZE	NI	NS	NM	NM	NB	NB
ZE	PB	PM	PM	PS	PI	ZE	NI	NS	NM	NM	NB
PI	PB	PB	PM	PM	PS	PI	ZE	NI	NS	NM	NM
PS	PB	PB	PB	PM	PM	PS	PI	ZE	NI	NS	NM
PM	PH	PB	PB	PB	PM	PM	PS	PI	ZE	NI	NS
PB	PH	PH	PB	PB	PB	PM	PM	PS	PI	ZE	NI
PH	PH	PH	PH	PB	PB	PB	PM	PM	PS	PI	ZE

Table 2 Look-up table for the fuzzy control

$\dot{\bar{\chi}}$ \ $\bar{\chi}$	1.0	0.8	0.6	0.5	0.2	0	−0.2	−0.5	−0.6	−0.8	−1.0
−1.0	0.0	−0.05	−0.2	−0.5	−0.7	−0.8	−0.9	−0.95	−1.0	−1.0	−1.0
−0.8	0.05	0.0	−0.05	−0.2	−0.5	−0.7	−0.8	−0.9	−0.95	−1.0	−1.0
−0.6	0.2	0.05	0.0	−0.05	−0.2	−0.5	−0.7	−0.8	−0.9	−0.95	−1.0
−0.5	0.5	0.2	0.05	0.0	−0.05	−0.2	−0.5	−0.7	−0.8	−0.9	−0.95
−0.2	0.7	0.5	0.2	0.05	0.0	−0.05	−0.2	−0.5	−0.7	−0.8	−0.9
0	0.8	0.7	0.5	0.2	0.05	0.0	−0.05	−0.2	−0.5	−0.7	−0.8
0.2	0.9	0.8	0.7	0.5	0.2	0.05	0.0	−0.05	−0.2	−0.5	−0.7
0.5	0.95	0.9	0.8	0.7	0.5	0.2	0.05	0.0	−0.05	−0.2	−0.5
0.6	1.0	0.95	0.9	0.8	0.7	0.5	0.2	0.05	0.0	−0.05	−0.2
0.8	1.0	1.0	0.95	0.9	0.8	0.7	0.5	0.2	0.05	0.0	−0.05
1.0	1.0	1.0	1.0	0.95	0.9	0.8	0.7	0.5	0.2	0.05	0.0

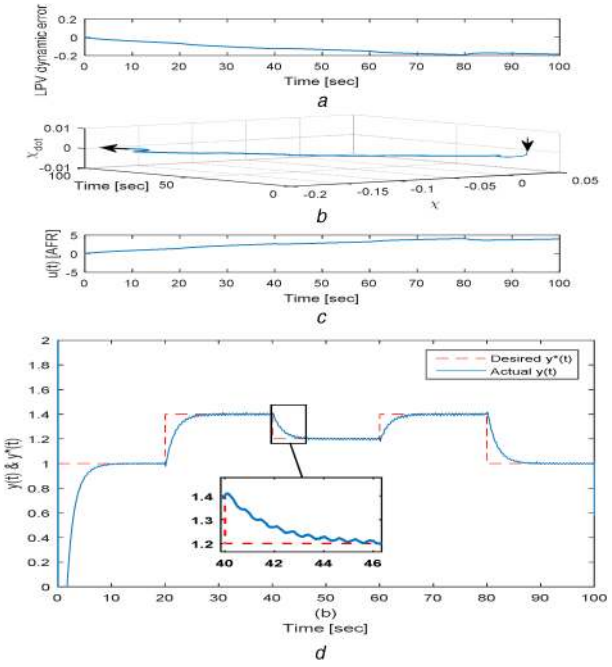

Fig. 5 *AFR system response with periodic disturbances under the proposed LPV-based fuzzy control*

$$\dot{V}(t) = \bar{\chi}(t)\dot{\bar{\chi}}(t) = g_{\dot{\chi}}\bar{\chi}(t)\left\{\begin{array}{l} a_{11}(\tau)\eta(t) + a_{12}\zeta(t) + \phi_\eta(t) + \Phi(s)\dot{y}^*(t) \\ -\Phi(s)\left[a_{21}(\tau)\eta(t) + a_{22}(\tau)\zeta(t) + \beta u(t) + \phi_\zeta(t)\right] \end{array}\right\} \quad (18)$$

Then, substituting (14) and (16) into (18) yields:

$$\begin{aligned} \dot{V}(t) &= \bar{\chi}(t)\dot{\bar{\chi}}(t) \\ &= g_\chi\bar{\chi}(t)[f(t) - \Phi(s)\beta g_u\Delta(t)\mathrm{sgn}(\bar{\chi}_\tau(t))] \\ &= g_\chi\bar{\chi}(t)f(t) - g_\chi\bar{\chi}(t)\Phi(s)\beta g_u\Delta(t)\mathrm{sgn}(\bar{\chi}(t)) \\ &\quad -g_\chi\bar{\chi}(t)\Phi(s)\beta g_u\Delta(t)[\mathrm{sgn}(\bar{\chi}_\tau(t)) - \mathrm{sgn}(\bar{\chi}(t))] \end{aligned} \quad (19)$$

If the LPV dynamic error manifold is outside of the convex set Ω (see the following remark, i.e. $|\bar{\chi}(t)| > c_s(\tau_u)$, where $c_s(\tau_u)$ is a positive value dependent on the upper bound of time-varying delay (τ_u), then $\mathrm{sgn}(\bar{\chi}_\tau(t)) = \mathrm{sgn}(\bar{\chi}(t))$. Besides, $\Phi(s)\beta\Delta(t) > 0$ ($\Phi(s)\Delta(t) < 0$, and $\beta < 0$). Therefore, as the output scaling factor g_u meets the inequality in (15), (19) becomes

$$\begin{aligned} \dot{V}(t) &\le g_{\dot{\chi}}|\bar{\chi}(t)|[|f(t)| - \Phi(s)\beta g_u\Delta(t)] \\ &\le -\lambda|\bar{\chi}(t)| \end{aligned} \quad (20)$$

Since $\lambda > 0$, $\dot{V}(t)$ is negative definite. Thus, the LPV dynamic error is asymptotically stable, i.e. $\bar{\chi}(t) \to 0$ as $t \to \infty$. As $\bar{\chi}(t) \to 0$, it meets (6) and subsequently the desired error dynamics in (7) is achieved. As a result, the tracking error $e(t)$ is also asymptotically stable. Moreover, the solution of inequality in (20) for the initial time t_0 and the initial value $\bar{\chi}(t_0)$ can be expressed as

$$t - t_0 \le \frac{(|\bar{\chi}(t_0)| - c_s(\tau_u))}{\lambda} \quad (21)$$

where t represents the time the operating point hits the boundary of the convex set of the LPV dynamic error manifold in (11), t_0 expresses the initial time and $t - t_0$ denotes the finite time to approach the convex set.

Remark: The convex set Ω of the LPV dynamic error is stated as $\Omega = \{\bar{\chi}(t)||\bar{\chi}(t)| \le c_s(\tau_u)\}$ where $c_s(\tau_u)$ is a positive value dependent on the upper bound of time-varying delay.

Finally, the procedure for the proposed LPV-based fuzzy control is summarised as follows:

Step 1: Design an LPV dynamic error as (6) and then determine the varying coefficients $p_j(\tau)$ and $q(\tau)$ based on the desired error dynamics (7).
Step 2: Calculate the difference between the LPV dynamic error values and substitute it in its derivative.
Step 3: Choose the input scaling factors, i.e. g_χ and $g_{\dot{\chi}}$ such that the values of the LPV dynamic error and its derivative are located in $[-1, 1]$.
Step 4: Select an output scaling factor g_u so that it satisfies the upper bound of inequality (15) for the stability requirement.
Step 5: Repeat Steps 2–4 to adjust control parameters g_χ, $g_{\dot{\chi}}$, and g_u if the output performance is not acceptable.

4 Simulation results and discussions

To verify the effectiveness, robustness, and performance of the proposed control scheme, the simulations under different operating conditions were conducted. The physical and suitable control parameters of an AFR dynamic model were considered as $\tau_s = 0.05$; $g_\chi = 0.5$; $g_{\dot{\chi}} = 0.05$; $g_u = 5000$; and $k_p = 0.01$. A set of delays with an increment of 0.1 s was conducted for $0.3\ \mathrm{s} \le \tau \le 2.7\ \mathrm{s}$. The external periodic disturbances were, respectively, chosen as $\phi_\eta(t) = 0.01\eta(t)\zeta(t)\cos(10t) - 0.05$ and $\phi_\zeta(t) = -0.05\sin(2t) + 0.6$. A desired second-order error dynamics $\ddot{e} + 1.4\dot{e} + e = 0$ was chosen, i.e. the system order $n = 1$, that yields $p_0(\tau) = -0.5\tau_s\tau$ and $q(\tau) = 1.4 + 0.5\tau$. Furthermore, the desired normalised AFR values were selected as 1, 1.2 and 1.4 during the different periods. In addition, the rich and lean AFR switching values were also chosen as 0.6 and 1.5.

The proposed LPV-based fuzzy control as expressed in (14) was applied to the internal dynamics of the AFR system with external periodic disturbances in (5). Fig. 5*a* displays the response of the LPV dynamic error which was converged towards a bounded set as expected (close to zero). The motion profile of the LPV dynamic error manifold in the phase plane was demonstrated (Fig. 5*b*). These results showed that the motion trajectory of the LPV dynamic error was asymptotically stable (its proof was given in Section 3.2). In addition, the AFR tracking error was asymptotically stable and followed the predefined desired error dynamics. Both input and output tracking are shown in Figs. 5*c* and *d*, respectively. It can be seen that the AFR tracking was satisfactory in the presence of external disturbances.

To further evaluate the extent of the robustness of the proposed control scheme, different levels of uncertainty in determining the time constant of the AFR internal dynamics were considered. Results showed that adding time constants higher than the actual time constant value lead to a little faster transient response and almost no change in the steady-state response (Fig. 6). Conversely, time constants lower than the actual value caused a slower transient response (the results are not shown). These results demonstrated that the proposed LPV-based fuzzy control scheme is not only effectively capable of stabilising the AFR system with a large time-varying delay but also it can compensate for external disturbances and high level of uncertainty in the system parameters.

In order to apply the proposed method in a practical setting, investigating the effect of saturation in control input is necessary. However, input saturation may make the system respond sluggish or may increase maximum overshoot which may result in system instability. In this simulation, as an initial step AFR of 3, i.e. 60% of the peak value in Fig. 5*d* was used as the saturation level. Fig. 7 represents the AFR system responses subject to a 50% time constant increase without and with input saturation. Evidently, the transient response under the saturation became sluggish. Likewise, Fig. 8 exhibits the same results under a 50% time constant decrease. Although the input saturation indeed resulted in a more sluggishness; they are still acceptable under the proposed LPV-based fuzzy control.

AFR is often run into the situation of the rich-lean-rich switching. Thus, the switching response was examined to evaluate

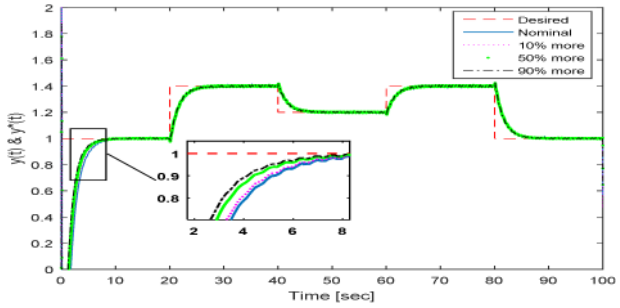

Fig. 6 *Output tracking subject to periodic disturbances and different levels of uncertainty in the time constant τ_s*

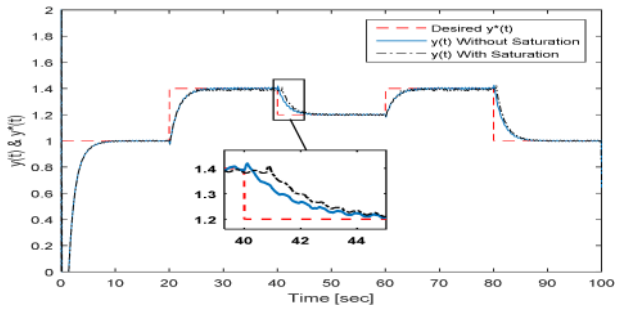

Fig. 7 *Output tracking response subject to a 50% increase in time constant τ_s without and with saturation*

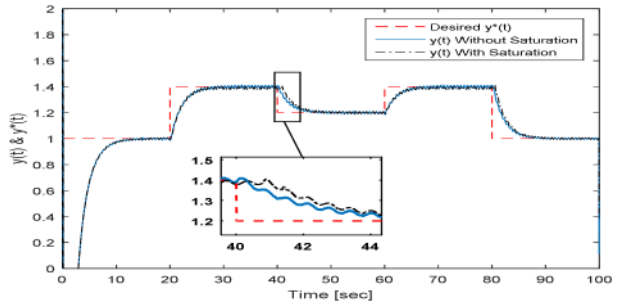

Fig. 8 *Output tracking response subject to a 50% decrease in the time constant τ_s without and with saturation*

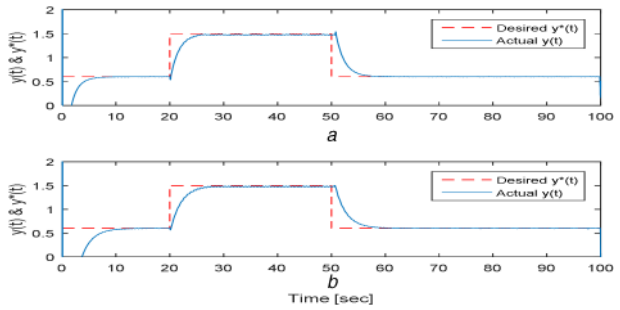

Fig. 9 *Rich-lean-rich AFR switching subject to the saturated control input with periodic disturbances*

(a) 50% increase, ***(b)*** 50% decrease of time constant τ_s

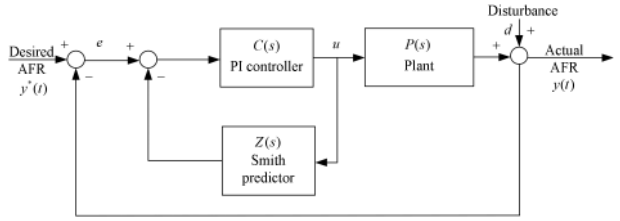

Fig. 10 *Block diagram of PI controller combined with Smith predictor*

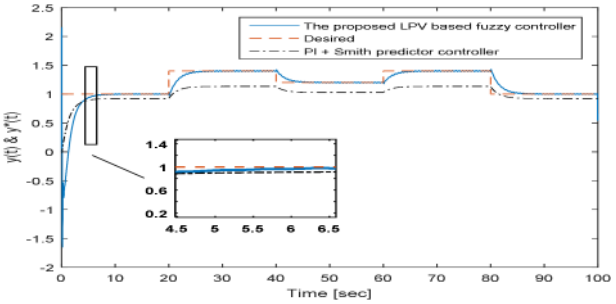

Fig. 11 *Comparing the PI controller combined with Smith predictor with the proposed LPV-based fuzzy control*

the performance of the proposed LPV-based fuzzy control (Fig. 9). The results showed that the tracking performance for rich-lean-rich AFR switching under a 50% more and less of a time constant was still satisfactory. Based on these results, it can be concluded that the proposed LPV-based fuzzy control can be effectively executed under different operating conditions.

In addition, the proposed control scheme was compared with a baseline controller, a proportional–integral (PI) controller $C(s) = k_p(1 + 1/Ts)$ combined with a parameter-varying Smith predictor, $Z(s) = 1/(\tau_s s + 1)(1 - e^{-\tau_s})$ (to compensate for the varying time-delay), where the parameter T is chosen equal to the time constant τ_s of the system. The control block diagram and compared response are, respectively, shown in Figs. 10 and 11. Fig. 11 shows that the baseline control always has a steady-state error for any proportional gain, k_p. These results revealed that the proposed LPV-based fuzzy controller indeed outperformed the baseline controller.

5 Conclusions

Tracking of desired AFR values through the proposed LPV-based fuzzy control for the internal dynamics of an AFR system is achieved. Owing to the non-minimum phase characteristic caused by the first-order Pade approximation of time-varying delay, the internal dynamics of the AFR system has an unstable state. The proposed solution scheme was: first, determine the LPV dynamic error consisting of the unstable system state and AFR tracking error with time-varying gains for handling both variables, i.e. unstable system state and AFR tracking error; and second, use a fuzzy control strategy to stabilise the LPV dynamic error. Results showed that both the unstable state and the AFR tracking error were stabilised when the proposed scheme was used. The closed-loop system stability was guaranteed through Lyapunov stability criteria. Finally, the simulation results demonstrated that the proposed LPV-based fuzzy control yielded a high level of robustness in spite of the presence of external disturbances, high level of uncertainties and saturated control input. Moreover, compared with a baseline controller, i.e. PI controller with Smith predictor also displayed its advantages. Further, the performance of rich-lean-rich AFR switching still remained satisfactory.

6 Acknowledgments

This work was supported by NPRP grant from the Qatar National Research Fund (a member of Qatar Foundation) [grant number 7-829-2-308].

7 References

[1] Lauber, J., Guerra, T.M., Dambrine, M.: 'Air-fuel ratio control in a gasoline engine', *Int. J. Syst. Sci.*, 2011, **42**, (2), pp. 277–286

[2] Muske, K.R., Jones, J.C.P., Franceschi, E.M.: 'Adaptive analytical model-based control for SI engine air–fuel ratio', *IEEE Trans. Control Syst. Technol.*, 2008, **16**, (4), pp. 763–768

[3] Tang, H., Weng, L., Dong, Z.Y., *et al.*: 'Adaptive and learning control for SI engine model with uncertainties', *IEEE/ASME Trans. Mechatronics*, 2009, **14**, (1), pp. 93–104

[4] Yildiz, Y., Annaswamy, A.M., Yanakiev, D., *et al.*: 'Spark ignition engine air-to-fuel ratio control: an adaptive control approach', *Control Eng. Pract.*, 2010, **18**, (12), pp. 1369–1378

[5] Chen, X., Wang, Y., Haskara, I., *et al.*: 'Optimal air-to-fuel ratio tracking control with adaptive biofuel content estimation for LNT regeneration', *IEEE Trans. Control Syst. Technol.*, 2014, **22**, (2), pp. 428–439
[6] Kahveci, N.E., Impram, S.T., Umut Genc, A.: 'Adaptive internal model control for air-fuel ratio regulation'. IEEE Intelligent Vehicles Symp., Dearborn, MI, USA, 2014, pp. 1091–1096
[7] Rupp, D., Guzzella, L., Haskara, I., *et al.*: 'Adaptive internal model control with application to fueling control', *Control Eng. Pract.*, 2010, **18**, (8), pp. 873–881
[8] Khajorntraidet, C., Ito, K., Shen, T.: 'Adaptive time delay compensation for air-fuel ratio control of a port injection SI engine'. 54th SICE, Hangzhou, China, 2015, pp. 1341–1346
[9] Choi, S.B., Hedrick, J.K.: 'An observer-based controller design method for improving air/fuel characteristics of spark ignition engines', *IEEE Trans. Control Syst. Technol.*, 1998, **6**, (3), pp. 324–334
[10] Zhang, X., Tsiotras, P., Knospe, C.: 'Stability analysis of LPV time-delayed systems', *Int. J. Control*, 2002, **75**, (7), pp. 538–558
[11] Zhang, F., Grigoriadis, K.M., Franchek, M.A., *et al.*: 'Linear parameter-varying lean burn air-fuel ratio control for a spark ignition', *J. Dyn. Syst. Meas. Control*, 2007, **129**, (4), pp. 404–414
[12] Ebrahimi, B., Tafreshi, R., Masudi, H., *et al.*: 'A parameter-varying filtered PID strategy for air-fuel ratio control of spark ignition engines', *Control Eng. Pract.*, 2012, **20**, (8), pp. 805–815
[13] Ebrahimi, B., Tafreshi, R., Mohammadpour, J., *et al.*: 'Second-order sliding mode strategy for air-fuel ratio control of lean-burn SI engines', *IEEE Trans. Control Syst. Technol.*, 2014, **22**, (4), pp. 1374–1384
[14] Postma, M., Nagamune, R.: 'Air-fuel ratio control of spark ignition engines using a switching LPV controller', *IEEE Trans. Control Syst. Technol.*, 2012, **20**, (5), pp. 1175–1187
[15] Tafreshi, R., Ebrahimi, B., Mohammadpour, J., *et al.*: 'Linear dynamic parameter-varying sliding manifold for air-fuel ratio control in lean-burn engines', *IET Control Theory Appl.*, 2013, **7**, (10), pp. 1319–1329
[16] Yin, H., Liu, Z.: 'Fuel-air ratio control for a spark ignition engine using gain-scheduled delay-dependent approach', *IET Control Theory Appl.*, 2015, **9**, (12), pp. 1810–1820
[17] Zope, R., Mohammadpour, J., Grigoriadis, K., *et al.*: 'Identification of air-fuel ratio dynamics in SI engines using linear parameter varying techniques'. Control and Applications Conf., Vancouver, Canada, 2011, pp. 120–125
[18] Wang, S., Yu, D.L.: 'A new development of internal combustion engine air-fuel ratio control with second-order sliding mode', *J. Dyn. Syst. Meas. Control*, 2007, **129**, (6), pp. 757–766
[19] Kahveci, N.E., Jankovic, M.J.: 'Adaptive controller with delay compensation for air-fuel ratio regulation in SI engines'. American Control Conf., Baltimore, MD, USA, 2010, pp. 2236–2241
[20] Benvenuti, L., Di Benedetto, M.D., Di Gennaro, S., *et al.*: 'Individual cylinder characteristic estimation for a spark injection engine', *Automatica*, 2003, **39**, pp. 1157–1169
[21] Fiengo, G., Grizzle, J.W., Cook, J.A., *et al.*: 'Dual-UEGO active catalyst control for emissions reduction: design and experimental validation', *IEEE Trans. Control Syst.*, 2005, **13**, (5), pp. 722–736
[22] Guzzella, L., Onder, H.C.: '*Introduction to modeling and control of internal combustion engine systems*' (Springer, Berlin, Germany, 2010, 2nd edn.)
[23] Hwang, C.L., Chang, L.J., Yu, Y.S.: 'Network-based fuzzy decentralized sliding-mode control for car-like mobile robots', *IEEE Trans. Ind. Electron.*, 2007, **54**, (1), pp. 574–585